

## **General Disclaimer**

### **One or more of the Following Statements may affect this Document**

- This document has been reproduced from the best copy furnished by the organizational source. It is being released in the interest of making available as much information as possible.
- This document may contain data, which exceeds the sheet parameters. It was furnished in this condition by the organizational source and is the best copy available.
- This document may contain tone-on-tone or color graphs, charts and/or pictures, which have been reproduced in black and white.
- This document is paginated as submitted by the original source.
- Portions of this document are not fully legible due to the historical nature of some of the material. However, it is the best reproduction available from the original submission.

A Three Parameter Analytic Phase Function  
for Multiple Scattering Calculations

by

George W. Kattawar

Report No. 13

The research described in this report  
was funded by the

National Aeronautics and Space  
Administration

Contract No. NGR 44-001-117

Department of Physics  
Texas A&M University  
College Station, Texas 77843

September 26, 1974

(NASA-CR-140998) A THREE PARAMETER  
ANALYTIC PHASE FUNCTION FOR MULTIPLE  
SCATTERING CALCULATIONS (Texas A&M Univ.)  
25 p HC \$3.25 CSCL 12A



N75-12674

Unclas  
63/64 02855

A paper based on the material in this report has been submitted to the  
Journal of Quantitative Spectroscopy and Radiative Transfer.

A Three Parameter Analytic Phase Function  
for Multiple Scattering Calculations

George W. Kattawar

Department of Physics  
Texas A&M University  
College Station, Texas 77843  
U. S. A.

Abstract:

A very simple procedure has been developed to fit the first three moments of an actual phase function with a three parameter analytic phase function. The exact Legendre Polynomial decomposition of this function is known which makes it quite suitable for multiple scattering calculations. The use of this function can be expected to yield excellent flux values at all depths within a medium. Since it is capable of reproducing the glory it can be used in synthetic spectra computations from planetary atmospheres. Accurate asymptotic radiance values can also be achieved as long as the single scattering albedo  $\omega_0 \geq 0.9$ .

## I. Introduction

One of the most widely used analytic phase functions in radiative transfer theory is that of Henyey and Greenstein.<sup>(1)</sup> Their function is specified in terms of a single parameter, called the asymmetry parameter, usually denoted by  $g$ , and has a simple Legendre polynomial decomposition. This function is given by

$$\phi(\mu, g) = (1-g^2)/[4\pi (1-2g\mu+g^2)^{3/2}] \quad (1)$$

where  $\mu$  is the cosine of the scattering angle  $\Theta$  and

$$g = \langle \mu \rangle = \int_0^{2\pi} \int_{-1}^1 \mu \phi(\mu, g) d\mu d\phi \quad (2)$$

This function has the following normalization

$$\int_0^{2\pi} \int_{-1}^1 \phi(\mu, g) d\mu d\phi = 1. \quad (3)$$

Now using the generating function for the Legendre polynomials, namely

$$(1-2g\mu + g^2)^{-1/2} = \sum_{n=0}^{\infty} g^n P_n(\mu), \quad |g| < 1 \quad (4)$$

and differentiating with respect to  $\mu$ , it is easy to show that

$$\phi(\mu, g) = \frac{1}{4\pi} \sum_{n=0}^{\infty} g^n (2n+1) P_n(\mu). \quad (5)$$

Defining

$$\langle P_n(\mu) \rangle = \int_0^{2\pi} \int_{-1}^1 P_n(\mu) \phi(\mu, g) d\mu d\phi \quad (6)$$

and using the fact that

$$\int_{-1}^1 P_n(\mu) P_m(\mu) d\mu = \frac{2}{2n+1} \delta_{nm} \quad (7)$$

we get

$$\langle P_n(\mu) \rangle = g^n \quad (8)$$

One of the major disadvantages of this single term phase function is that it can't produce the familiar glory which is almost always prevalent in realistic phase functions computed from Mie Theory. This is of major importance when one is computing synthetic spectra in planetary atmospheres. This fact was pointed out by Whitehill and Hansen<sup>(2)</sup> to explain the so called inverse phase effect on Venus. To produce the glory phenomena requires the use of a superposition of two Henyey-Greentstein phase functions. This was done by Irvine<sup>(3)</sup> who used

$$\phi(\mu, g_1, g_2, \alpha) = \alpha \phi(\mu, g_1) + (1-\alpha)\phi(\mu, g_2) \quad (9)$$

However, Irvine only fit the first moment of the phase function. It is the purpose of this paper to show how the parameters  $g_1$ ,  $g_2$ , and  $\alpha$  can be computed very simply to fit at least three moments of the phase function thus allowing more accurate flux and internal radiance calculations. Hereafter the function defined by equation (1) will be referred to as OTHG (one term Henyey-Greenstein) and that defined by (9) as TTHG (two term Henyey-Greenstein).

## 2. Theory

### 2.1 Moment Fitting

Let us assume that we are given the first three components of the projection of a realistic phase function on a basis of Legendre polynomials and label them  $g$ ,  $h$ , and  $t$  respectively. This is equivalent to knowing the first three moments. From equations (5) and (9) it follows that

$$\phi(\mu, g_1, g_2, \alpha) = \frac{1}{4\pi} \sum_{n=0}^{\infty} (\alpha g_1^n + (1-\alpha)g_2^n) (2n+1) P_n(\mu) \quad (10)$$

and

$$\langle P_n(\mu) \rangle = \alpha g_1^n + (1-\alpha)g_2^n \quad (11)$$

We can now set up the following three equations

$$\alpha g_1 + (1-\alpha)g_2 = g \quad (12)$$

$$\alpha g_1^2 + (1-\alpha)g_2^2 = h \quad (13)$$

$$\alpha g_1^3 + (1-\alpha)g_2^3 = t \quad (14)$$

These equations can readily be solved yielding

$$g_2 = t - hg - [(hg-t)^2 - 4(h-g^2)(tg-h^2)]^{1/2} / 2(h-g^2) \quad (15)$$

$$g_1 = (gg_2 - h) / (g_2 - g) \quad (16)$$

$$\alpha = (g - g_2) / (g_1 - g_2) \quad (17)$$

The minus sign was chosen so that  $g_2$  could become negative. If one chooses the plus sign for the square root in equation (15) then one obtains  $g_1$ . It should be noted here that there is nothing in these equations to prevent  $|g_2| > 1$ . Although this case is the exception rather than the rule we will show how to deal with it later.

## 2.2 Internal Radiance from Eigenvalue Expansion

Van de Hulst<sup>(4)</sup> derived an expression for the asymptotic internal radiance in a homogeneous medium in terms of a perturbation expansion involving an eigenvalue along with  $g$  and  $h$ . We will extend the perturbation expansion to also include  $t$  and thus show that a better fit can be obtained. We will adopt the notation of van de Hulst to avoid any confusion to the reader. The basic assumption is that the intensity deep inside a medium and far away from a lower boundary can be expressed as

$$I(\tau\mu) \propto e^{-k\tau} P(\mu), \quad -1 \leq \mu \leq 1 \quad (18)$$

where  $\tau$  is the optical depth measured from the top of the medium and  $k$  is the smallest eigenvalue of the equation

$$(1-k\mu) P(\mu) = \frac{\omega_0}{2} \int_{-1}^1 h(\mu, \mu') P(\mu') d\mu' \quad (19)$$

where

$$h(\mu, \mu') = \int_0^{2\pi} \phi[\mu\mu' + (1-\mu^2)^{1/2} (1-\mu'^2)^{1/2} \cos(\phi-\phi')] d\phi \quad (20)$$

and  $\omega_0$  is the single scattering albedo.

This assumption has been checked numerically by Plass et al.<sup>(5)</sup> and was shown to be quite valid for  $\omega_0 \sim 1$ . The exponential behavior has also been demonstrated exactly by a solution to the one dimensional problem (Kattawar and Plass<sup>(6)</sup>).

Van de Hulst obtains the following series expansions for  $\omega_0$  and  $P(\mu)$ ;

$$\omega_0 = 1 - \frac{1}{3(1-g)}k^2 - \frac{4-9g+5gh}{45(1-g)^3(1-h)}k^4 + O(k^6) \quad (21)$$

$$P(\mu) = 1 + \frac{1}{1-g}kP_1(\mu) + \frac{2}{3(1-g)(1-h)}k^2P_2(\mu) + O(k^3) \quad (22)$$

Since we have demonstrated a method of fitting a phase function up to the term for  $P_3(\mu)$ , we must extend the perturbation series for  $P(\mu)$  up to this term. This can be done in a rather straightforward manner and we obtain

$$P(\mu) = 1 + \frac{1}{1-g} k P_1(\mu) + \frac{2}{3(1-g)(1-h)} k^2 P_2(\mu) + \frac{2}{5(1-g)(1-h)(1-t)} k^3 P_3(\mu) + O(k^4) \quad (23)$$

The coefficient of  $k^6$  in  $\omega_0$  will involve  $\langle P_4(\mu) \rangle$  and we will not include it. It is thus clear that by using the three parameter phase function that more accurate internal radiances will be obtained since the OTHG only fits  $g$ . It should be noted, however, that all higher values of  $\langle P_n(\mu) \rangle$  are given by  $g^n$  for the OTHG. In order to carry out the expansion given by equation (23) we must be able to determine the eigenvalue  $k$ .

### 2.3 Eigenvalue Computation

The eigenvalues can be computed from equation (19). The proof that the eigenvalues are real was given by Kuscer and Vidav<sup>(7)</sup>. The integral was discretized by using a twenty eight point Lobatto quadrature. Now equation (19) can easily be manipulated so that one can solve for  $k^2$  rather than  $k$  since it is well known that the eigenvalues occur in pairs  $(\pm k)$ . The program was tested by using the isotropic phase function ( $g=0$ ) and computing the eigenvalues for several values of  $\omega_0$ . The results were compared to those given by van de Hulst<sup>(8)</sup> for this case and agreement was achieved to every figure given.

### 3. Numerical Results

The first thing to be tested was how well the eigenvalues computed by the OTHG and the TTHG compared to the eigenvalues of an actual phase function. The phase function was computed using the Haze L distribution of Deirmendjian<sup>(9)</sup> which is a modified gamma distribution of the form

$$n(r) \propto r^2 e^{-15.1186r^{1/2}} \quad (24)$$

The refractive index used was  $N = 1.55 - 0.0i$  typical of atmospheric aerosols for a wavelength of  $0.55 \mu\text{m}$ . The resulting phase function is shown in Figure 1 along with the OTHG and TTHG which were computed from the appropriate values of  $\langle P_n \rangle$ . The values of  $\langle P_n \rangle$ , ( $n = 1, 2, 3$ ) were computed in two ways. First a numerical integration was performed over the phase function computed at very small angular intervals. Secondly these values can also be obtained directly from the  $\Lambda$  coefficients (See Kattawar et al.<sup>(10)</sup>) by

$$\begin{aligned} \langle P_n \rangle = \frac{4\pi}{2n+1} & \left[ \frac{(n+1)(n+2)}{(2n+3)(2n+5)} \Lambda_{n+2}^1 + \frac{6n^2 + 6n - 4}{(2n-1)(2n+3)} \Lambda_n^1 \right. \\ & \left. + \frac{n(n-1)}{(2n-3)(2n-1)} \Lambda_{n-2}^1 + \frac{2(n+1)}{(2n+3)} \Lambda_{n+1}^3 + \frac{2n}{(n-1)} \Lambda_{n-1}^3 \right] \end{aligned} \quad (25)$$

Excellent agreement was obtained between the two methods. It should be noted from Figure 1 that the TTHG not only provides a better approximation to the glory ( $\theta=180^\circ$ ) but also a better approximation to the diffraction peak ( $\theta=0^\circ$ ). Table 1 gives a comparison between the eigenvalues computed from a realistic phase function and those computed using a TTHG and a OTHG approximation to it. It should be emphasized, that only the smallest eigenvalue was chosen since this is the one that dominates the solution for large  $\tau$ . It should be noted that the TTHG provides excellent eigenvalue agreement for all values of  $\omega_0$  used.

As a further test we wanted to consider the efficacy of the method in determining internal radiance in optically deep homogeneous media. Our first test employed the well known Rayleigh phase function. Since  $g = 0$  for this function, the OTHG reduces to isotropic scattering; however,  $h = 0.1$  and the TTHG produces the curve shown in Figure 2. This is a much more realistic description of Rayleigh scattering than the OTHG. The asymptotic internal radiance for Rayleigh scattering has already been calculated by Plass, et al.<sup>(5)</sup> The eigenvalue for the case where  $\omega_0 = 0.9$  was computed both from equation (19) and by fitting the actual exponential fall off. Both calculations gave the same value for the eigenvalue



namely  $k = 0.5232$ . The values of  $k$  obtained by using the OTHG and the TTHG were 0.5254 and 0.5232, respectively. A comparison of the upward and downward internal radiance is shown in Figure 3. The radiance values presented for the OTHG and the TTHG were computed from equation (23) using the appropriate eigenvalues. As can be seen from the figure, the OTHG provides a better fit for  $0 \leq \mu \leq 0.2$  for the upward radiance but the TTHG is better for  $0.2 < \mu \leq 1.0$ . For the downward radiance the TTHG is better everywhere. It should also be noted that for values of  $\omega_0 \geq 0.9$  one can obtain quite excellent asymptotic internal radiances without doing very large scale computer calculations by simply using equation (23) with appropriate values of  $k$ ,  $g$ ,  $h$ , and  $t$ .

We next computed a phase function using the size distribution in equation (24) and a wavelength of  $0.55 \mu\text{m}$  for a refractive index of  $N=1.55-0.001i$ . This curve along with the OTHG and TTHG are shown in Figure 4. The asymptotic normalized radiances are shown in Figure 5. The difference between the actual asymptotic radiance and that computed with the TTHG using the parameters  $k$ ,  $g$ ,  $h$ ,  $t$ , in equation (23) is almost imperceptible on the scale of the figure. The OTHG internal radiances computed with the parameters  $k$ ,  $g$ ,  $g^2$ ,  $g^3$  is not quite as good. A more dramatic comparison can be seen in the following example. The size distribution was held fixed and the refractive index was changed to  $N=1.55-0.0127i$ . This gave the following set of curves shown in Figure 6. In Figure 7 we show a comparison of the asymptotic radiances computed using the matrix operator theory with the actual phase function compared to that for the TTHG and OTHG computed using equation (23). For the TTHG the parameters  $k$ ,  $g$ ,  $h$ , and  $t$  were used which agree with the actual phase function and for the OTHG the corresponding parameters were  $k$ ,  $g$ ,  $g^2$ , and  $g^3$ . It is easily seen that the TTHG provides a better approximation to the upward radiance. There is always more disagreement in the upward radiance as compared to the downward radiance, since the upward is derived from the downward. Although the curves shown for the TTHG and the OTHG were computed up to order  $k^3$ , the expansion can be extended to higher orders until convergence is

reached. This would give the true asymptotic limit since all values of  $\langle P_n \rangle$  are known for these two functions.

To test the TTHG on a phase function indicative of terrestrial clouds, we used the size distribution

$$n(r) \propto r^6 e^{-1.5r} \quad (26)$$

with  $N = 1.33 - 0.01$  for  $\lambda = 0.77 \mu m$ . The following values were obtained:

$g = 0.8479$ ,  $h = 0.7763$ , and  $t = 0.6523$ . Fitting these three values the TTHG gives  $g_1 = 0.8792$ ,  $g_2 = 0.9835$ , and  $\alpha = 0.9832$ . These results are presented in Figure 8 along with the OTHG. It is easily seen that the TTHG greatly overestimates the glory peak ( $\theta = 180^\circ$ ) even though this function has the same values of  $g$ ,  $h$ , and  $t$  as the actual phase function. If one, however, wants to tolerate a small error in  $t$  and fit the glory peak this can be done in the following way. We will still require that the TTHG fit both  $g$  and  $h$ , however, we will relax the requirement on fitting  $t$  in favor of fitting a particular value for the glory.

Therefore,

$$\alpha g_1 + (1-\alpha)g_2 = g \quad (27)$$

$$\alpha g_1^2 + (1-\alpha)g_2^2 = h \quad (28)$$

Eliminating  $g_1$  we get

$$g_2 = G - [\alpha(H-G^2)/(1-\alpha)]^{1/2} \quad (29)$$

$$g_1 = [G - (1-\alpha)g_2]/\alpha \quad (30)$$

Therefore by adjusting the ratio  $\alpha/(1-\alpha)$  we can reproduce the glory peak at the expense of introducing an error in  $t$ . This is shown in Figure 8. The exact value of  $t$  is 0.6523 and for the TTHG which fits the glory peak it is 0.6659 which is a 2 percent error. This should be contrasted to the OTHG which has a 7 percent error in  $h$  and a  $6\frac{1}{2}$  percent error in  $t$ . The major difference in the two TTHG phase functions only occurs for scattering angles greater than  $110^\circ$ . This demonstrates that the third moment of a phase function is quite sensitive to shape and one must be very careful in using phase functions which appear to

"look" similar to real phase functions. The technique just described is what one would use when a fit to  $g$ ,  $h$ , and  $t$  produces a value of  $|g_2| > 1$ . One would then have to sacrifice a fit to  $t$  in favor of a fit to the glory.

In order to study the effects of the approximate phase functions on the reflected intensity, we chose the following model:

$$n(r) \propto r^6 e^{-12r} \quad (31)$$

with a refractive index of  $N = 2.25 - 0.006i$  for a wavelength of  $0.565 \mu\text{m}$ . This phase function along with the OTHG and TTHG are shown in Figure 9. The single scattering albedo  $\omega_0 = 0.8943$ . In order that there be no scaling in optical depth we considered a homogeneous semi-infinite atmosphere. The matrix operator program was used to calculate the reflected radiances for the three phase functions.

In Figure 10 we see a comparison of the reflected radiance for  $\mu_0 = 1.0$  as a function of the cosine of the zenith angle. What is particularly striking is the degree to which single scattering features are carried over into the multiple scattering results. For example from Figure 9 we see that the TTHG crosses the actual phase function curve for angles  $\geq 90^\circ$  at two points corresponding to  $\mu = 0.24$  and  $0.91$ . These correspond very closely to the crossover points from Figure 10 for the multiple scattering results. The values in parentheses are the irradiance values and it can be seen that the TTHG gives only a 1 percent error in the irradiance while the OTHG gives a 7 percent error. Although the TTHG produces good values for the irradiance, the reflected radiance shows large discrepancies. Therefore if one needs precise values of the radiance then use of the analytic phase function can give errors which are quite large. Figure 11 is the same case as Figure 10 except  $\mu_0 = 0.1182$ . The radiance in the principal plane is shown ( $\phi = 0^\circ$  and  $180^\circ$ ). Again large discrepancies exist between the actual phase function results and the two analytic phase functions, however the flux value for the TTHG is in error by only 1 percent while the OTHG is in error by 5.5 percent.

#### 4. Conclusions

The use of this function can be expected to yield quite good asymptotic radiances in a medium whose single scattering albedo is  $\geq 0.9$ . We have shown that this function can yield quite accurate eigenvalues which govern the rate of decrease of the radiance and irradiance at asymptotic depths. This also implies its effectiveness in the computation of heating rates. It can also produce the familiar glory so often seen in realistic phase functions. This should be quite useful in the computations of synthetic spectra from planetary atmospheres where a parameterization of the phase function can be judiciously used. Although the values of the reflected radiance can be in error by a large percent, the reflected irradiance values can be quite accurate. Therefore this function can be effectively used whenever radiance values are averaged over certain intervals. This is precisely the case when we are computing synthetic spectra from various portions of a planetary atmosphere where averages are performed over portions of a planet covered by the spectrograph slit.

Bibliography

1. L. C. Henyey and J. L. Greenstein, *Astrophys. J.*, 93, 70 (1941).
2. L. P. Whitehill and J. E. Hansen, *Icarus*, to appear.
3. W. M. Irvine, *Astrophys. J.*, 4, 1563 (1965).
4. H. C. van de Hulst, *Bull. Astr. Inst. Netherlands* 20, 77 (1968).
5. G. N. Plass, G. W. Kattawar, and J. Binstock, *JQSRT* 13, 1081 (1973).
6. G. W. Kattawar and G. N. Plass, *JQSRT* 13, 1965 (1973).
7. I. Kuscer and I. Vidav, *J. Math. Anal. and Appl.* 25, 80 (1969).
8. H. C. van de Hulst, *J. Comp. Phys.* 3, 291 (1968).
9. D. Deirmendjian, *Electromagnetic Scattering on Spherical Polydispersions*, Elsevier, New York (1969).
10. G. W. Kattawar, S. J. Hitzfelder, and J. Binstock, *J. Atmos. Sci.* 30, 289 (1973).

### Figure Captions

- Fig. 1 Phase function as a function of scattering angle for a size distribution  $n(r) \propto r^2 e^{-15.1186r^{1/2}}$  with refractive index  $N = 1.55 - 0.0i$  at a wavelength of  $\lambda = 0.55\mu\text{m}$ . TTHG is the two term Henyey-Greenstein analytic phase function obtained by fitting the first three moments of the actual phase function and OTHG is the one term Henyey Greenstein phase function obtained by fitting only the first moment.
- Fig. 2 Same as Fig. 1, except the actual phase function is that for Rayleigh scattering.
- Fig. 3 Upward and downward normalized asymptotic internal radiances. The values of the single scattering albedo  $\omega_0$  were computed from equation (21) using the eigenvalues  $k$  computed from equation (19). These results are for the phase function used in Fig. 2.
- Fig. 4 Same as Fig. 1 except  $N = 1.55 - 0.001i$
- Fig. 5 Same as Fig. 3 except phase function used was that of Fig. 4.
- Fig. 6 Same as Fig. 1 except  $N = 1.55 - 0.0127i$
- Fig. 7 Same as Fig. 3 except phase function was that of Fig. 6.
- Fig. 8 Same as Fig. 1 except  $n(r) \propto r^6 e^{-1.5r}$  with  $N = 1.33 - 0.0i$  for  $\lambda = 0.70\mu\text{m}$ .
- Fig. 9 Same as Fig 7 except  $n(r) \propto r^6 e^{-12r}$  with  $N = 2.25 - 0.006i$  for  $\lambda = 0.565\mu\text{m}$ .
- Fig. 10 Reflected radiances as a function of the cosine of the zenith angle for a homogeneous semi-infinite atmosphere scattering according to the phase function for Fig. 9. Cosine of incident angle  $\mu_0 = 1.0$ .
- Fig. 11 Same as Fig. 10 except  $\mu_0 = 0.1882$  and the results are for the the principal plane  $\phi = 0^\circ$  and  $180^\circ$ .

TABLE 1.

Comparison of eigenvalues for a real phase function  
and those computed from the OTHG and the TTHG.

$\omega_0$	$k_E$	$k_{TTHG}$	% Error for TTHG	$k_{OTHG}$	% Error for OTHG
0.9999	0.01015	0.01015	0	0.01015	0
0.999	0.03209	0.03209	0	0.03209	0
0.99	0.1016	0.1016	0	0.1017	0.1
0.95	0.2284	0.2284	0	0.2296	0.23
0.90	0.3251	0.3251	0	0.3281	0.92
0.85	0.4006	0.4006	0	0.4054	1.20
0.80	0.4652	0.4652	0	0.4718	1.42
0.75	0.5227	0.5227	0	0.5310	1.59
0.65	0.6237	0.6238	0.02	0.6347	1.76
0.55	0.7115	0.7116	0.01	0.7241	1.77
0.45	0.7890	0.7892	0.02	0.8022	1.67
0.35	0.8575	0.8578	0.03	0.8701	1.47
0.25	0.9166	0.9173	0.08	0.9275	1.19
0.15	0.9648	0.9657	0.09	0.9724	0.79
0.05	0.9958	0.9965	0.07	0.9978	0.2

Figure 1

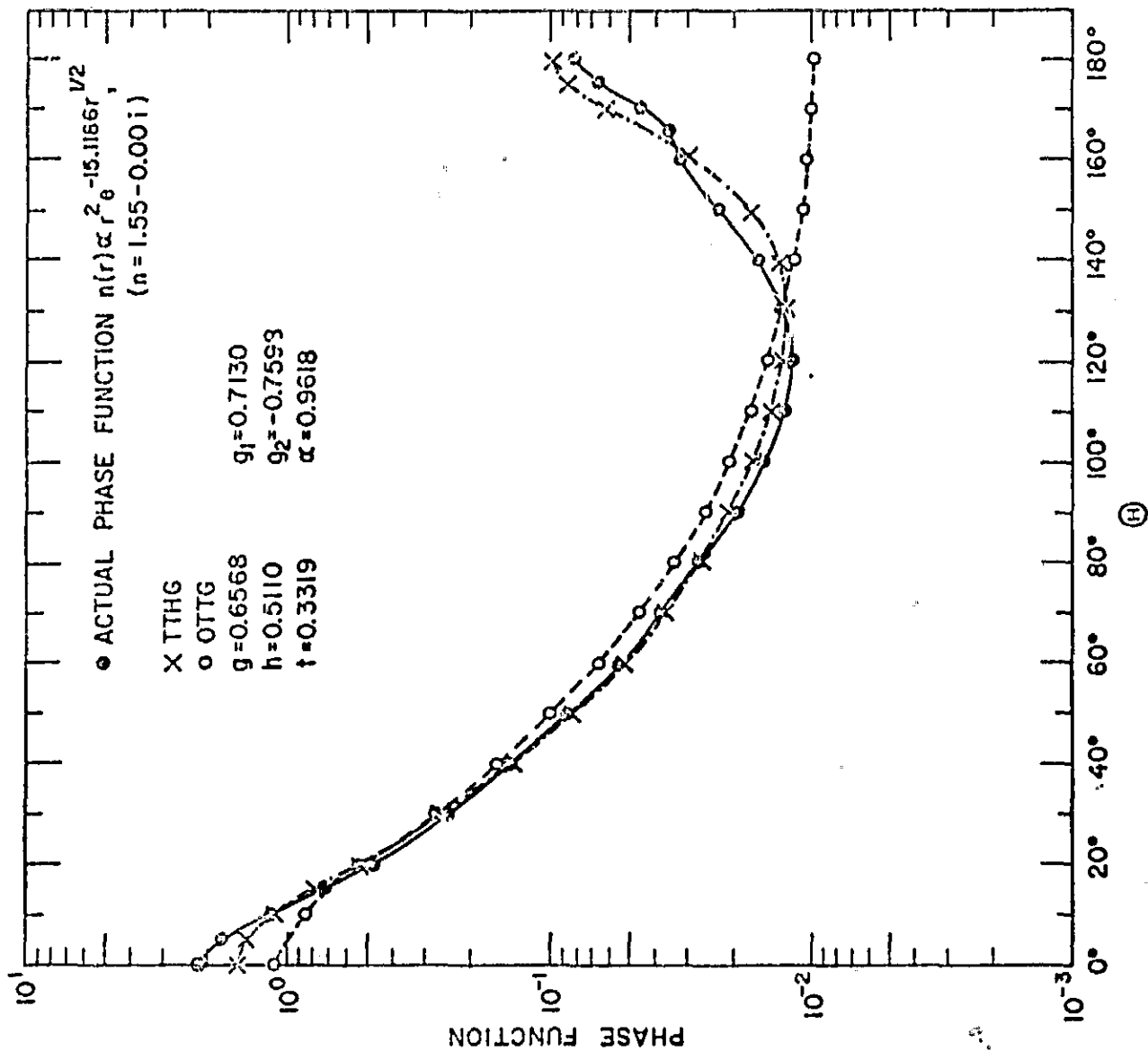




Figure 2

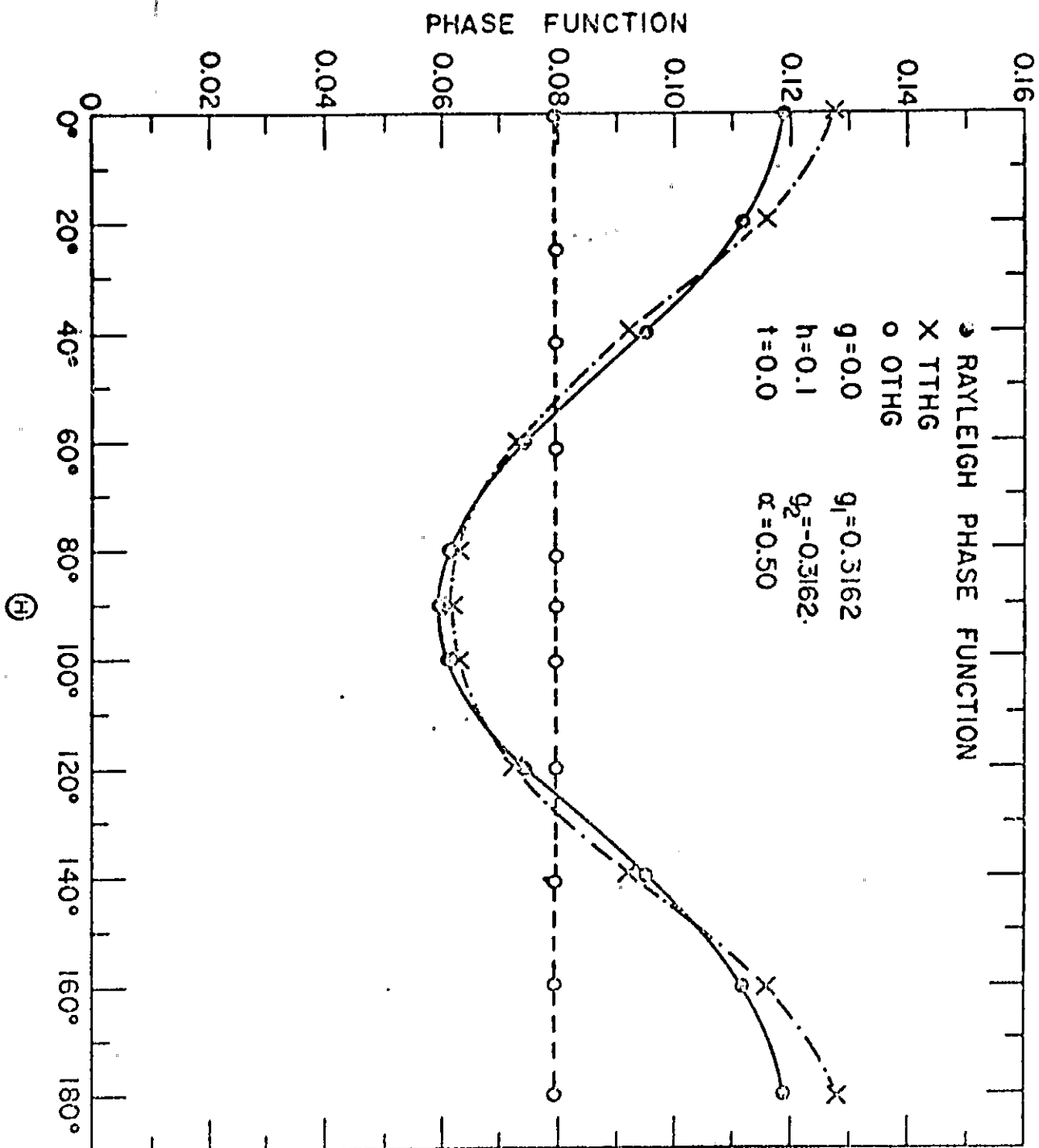
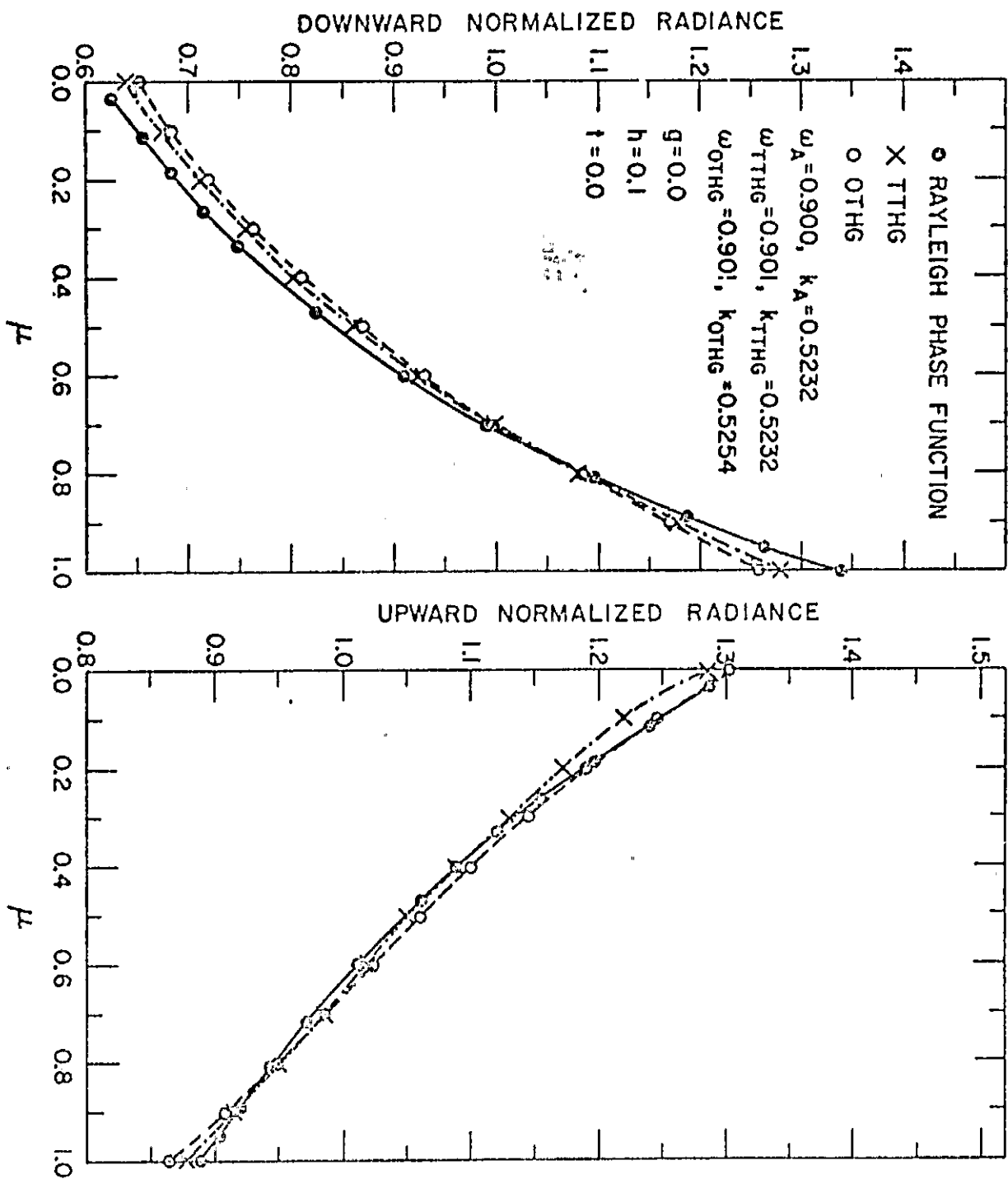


Figure 3



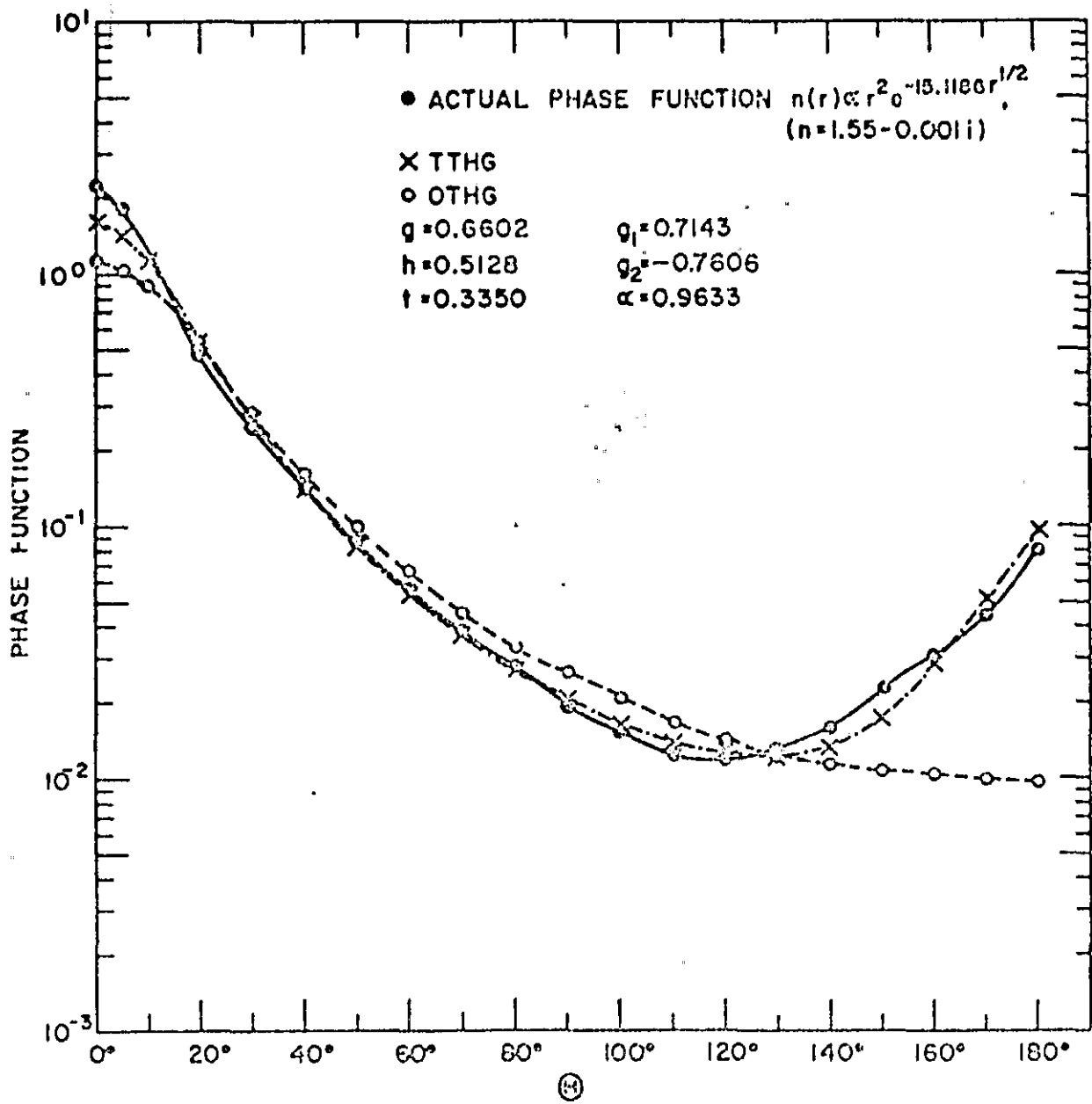


Figure 4

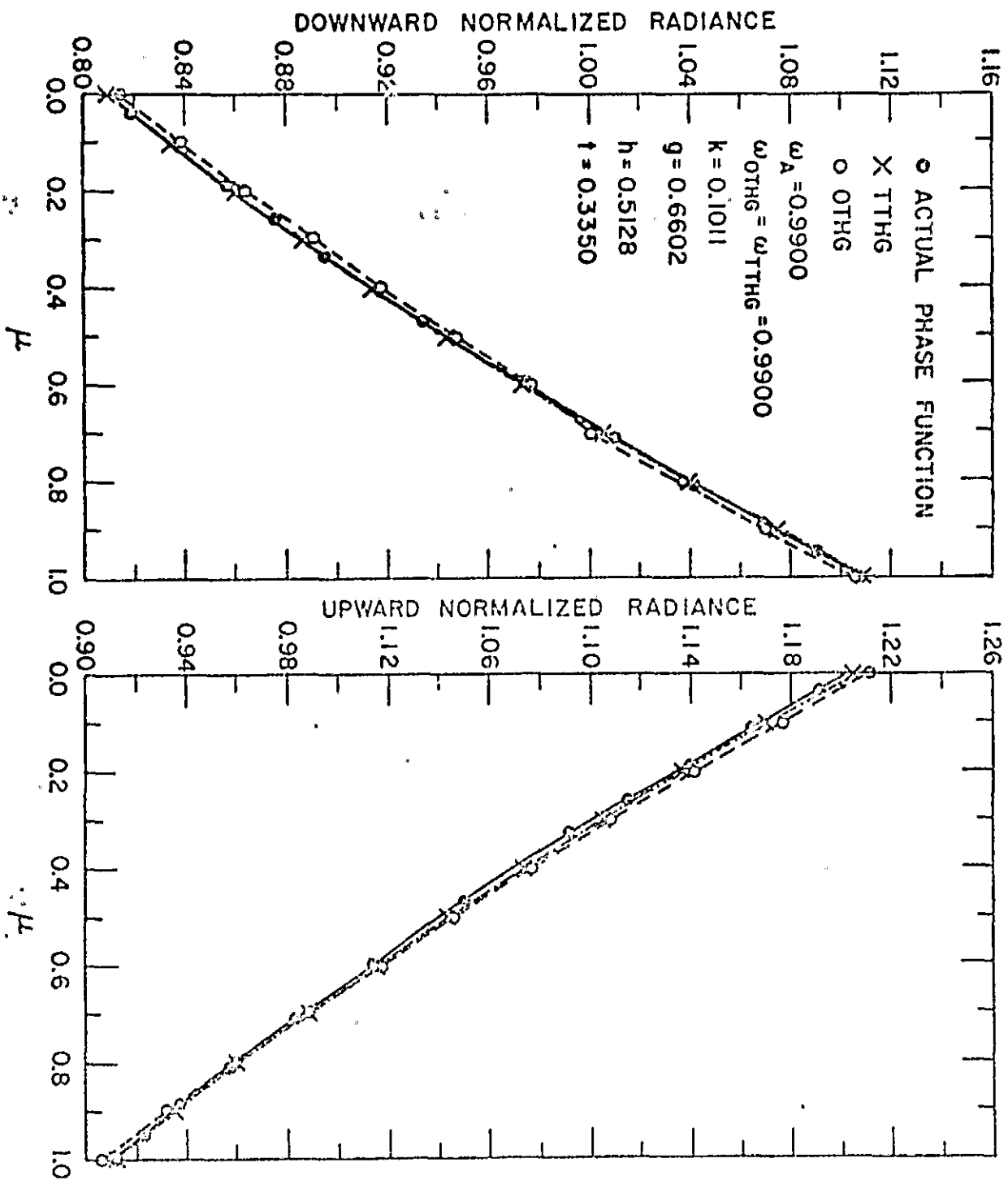


Figure 5

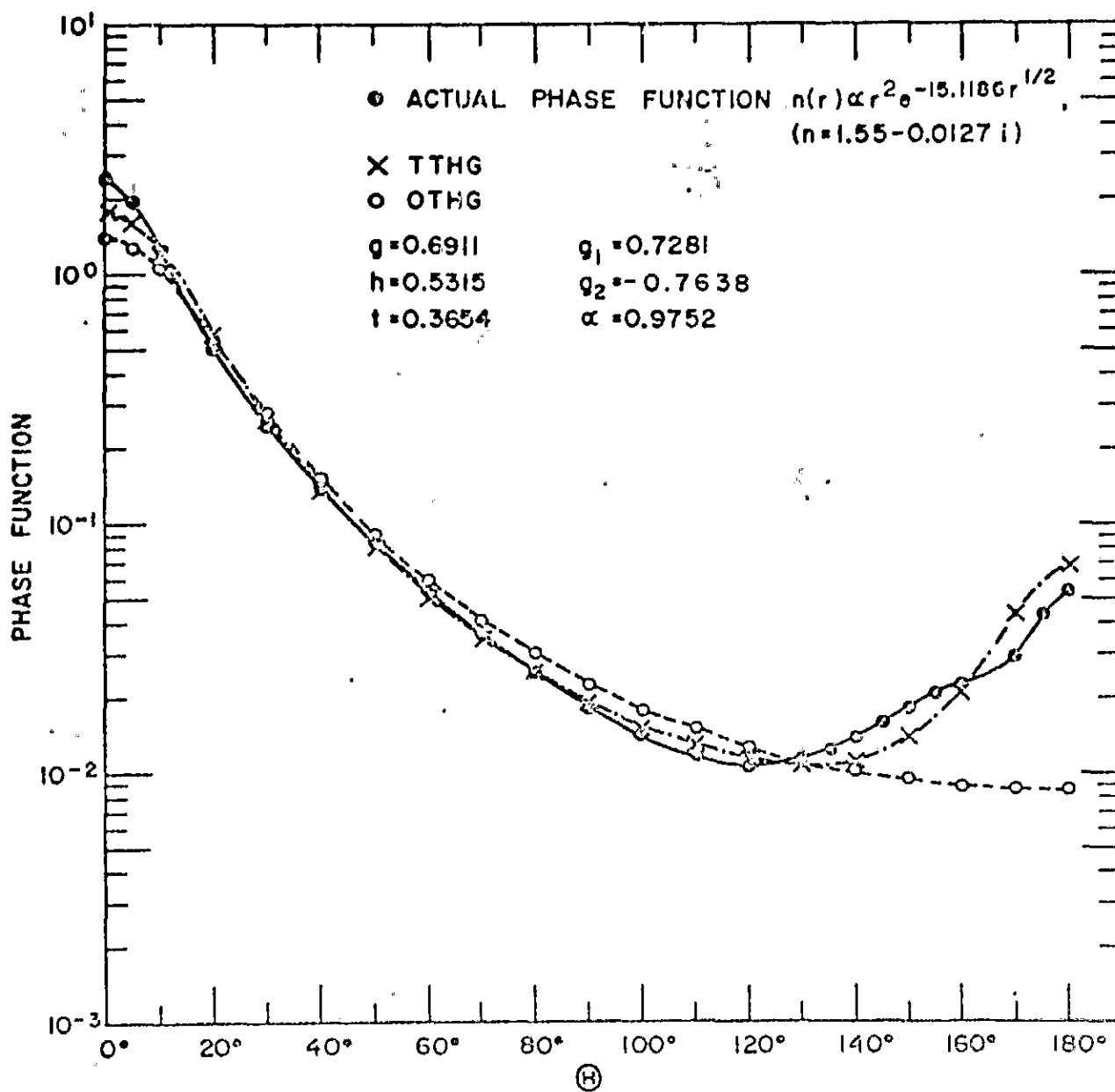
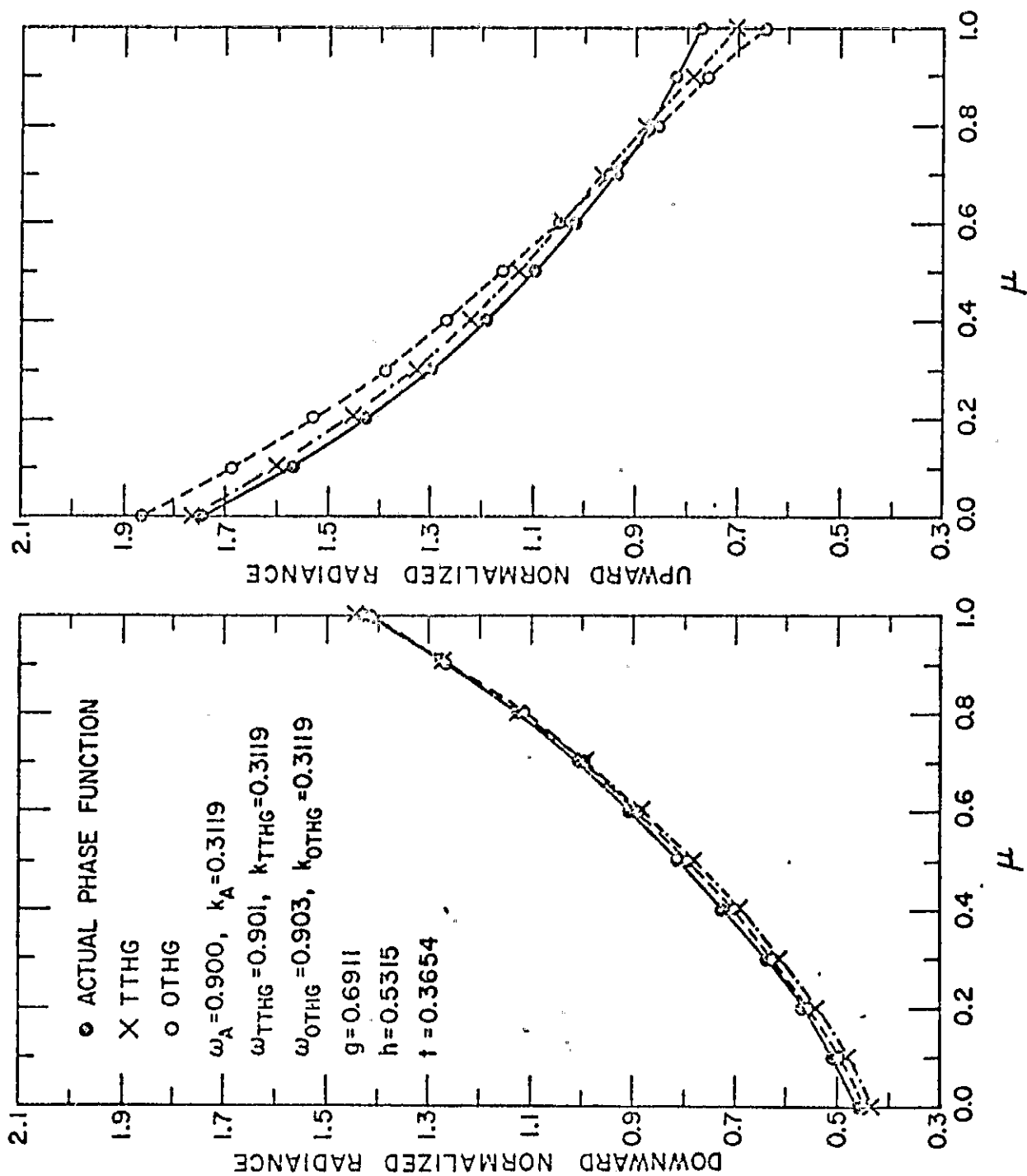


Figure 6

Figure 7



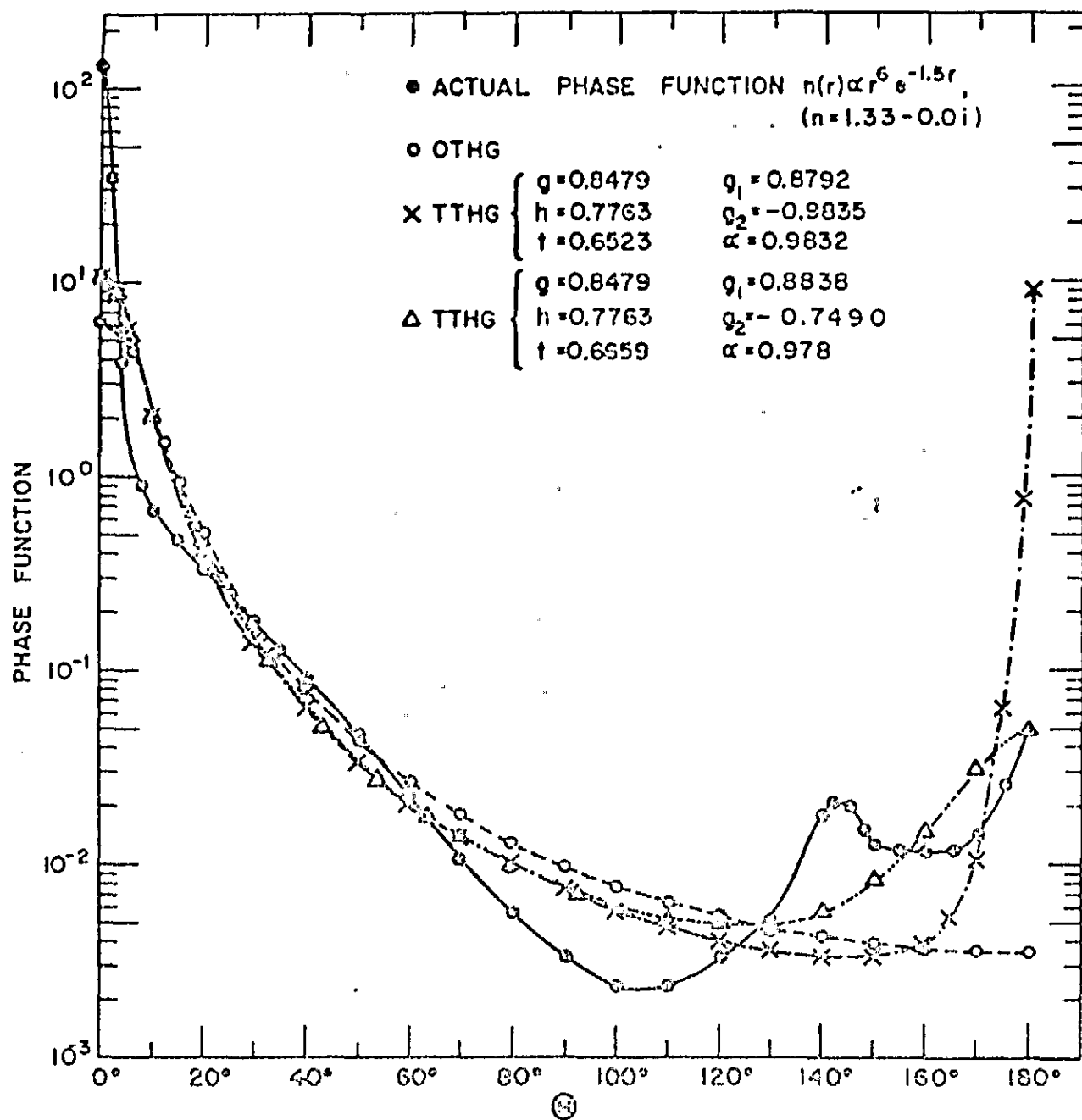
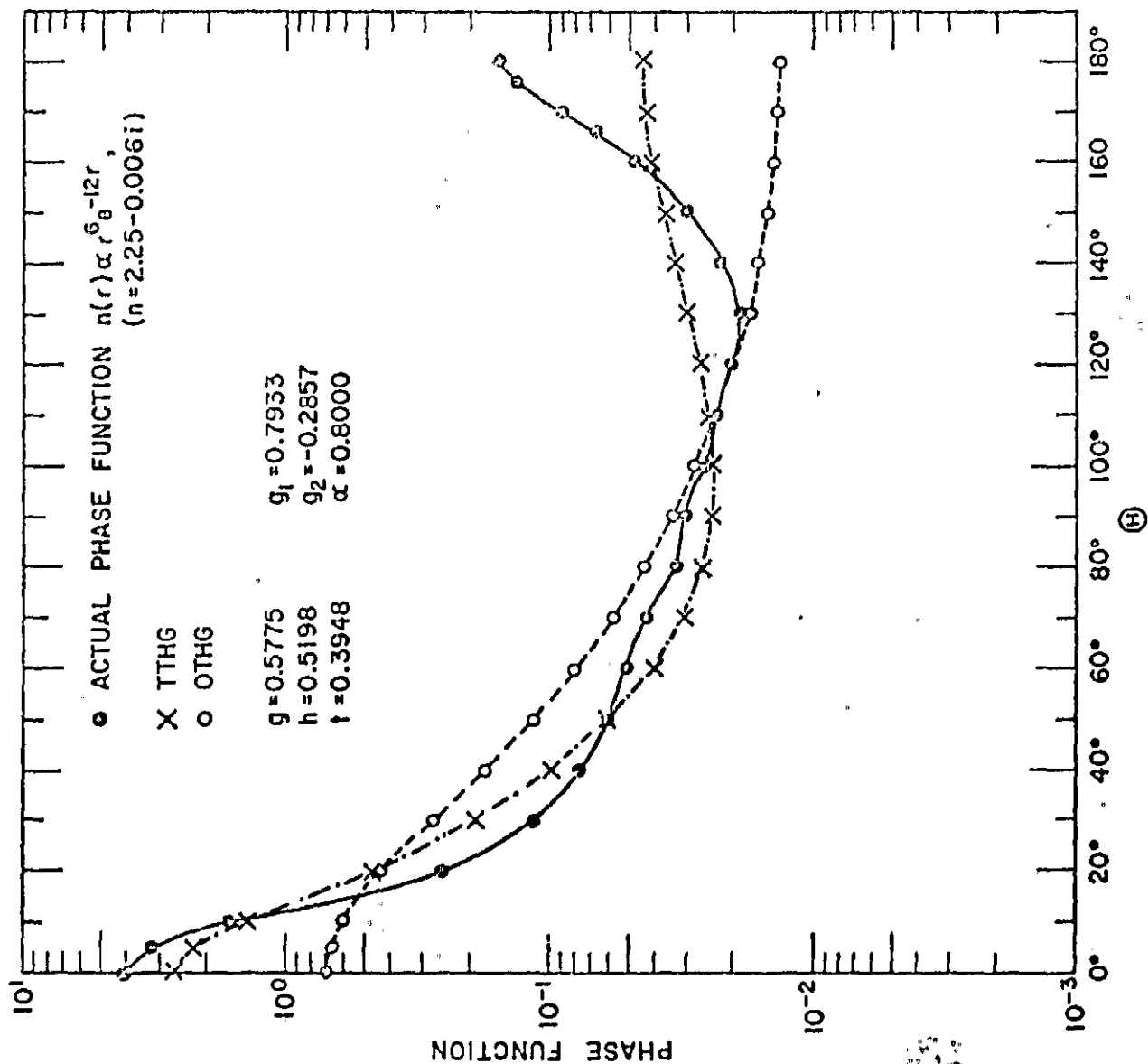


Figure 8

Figure 9





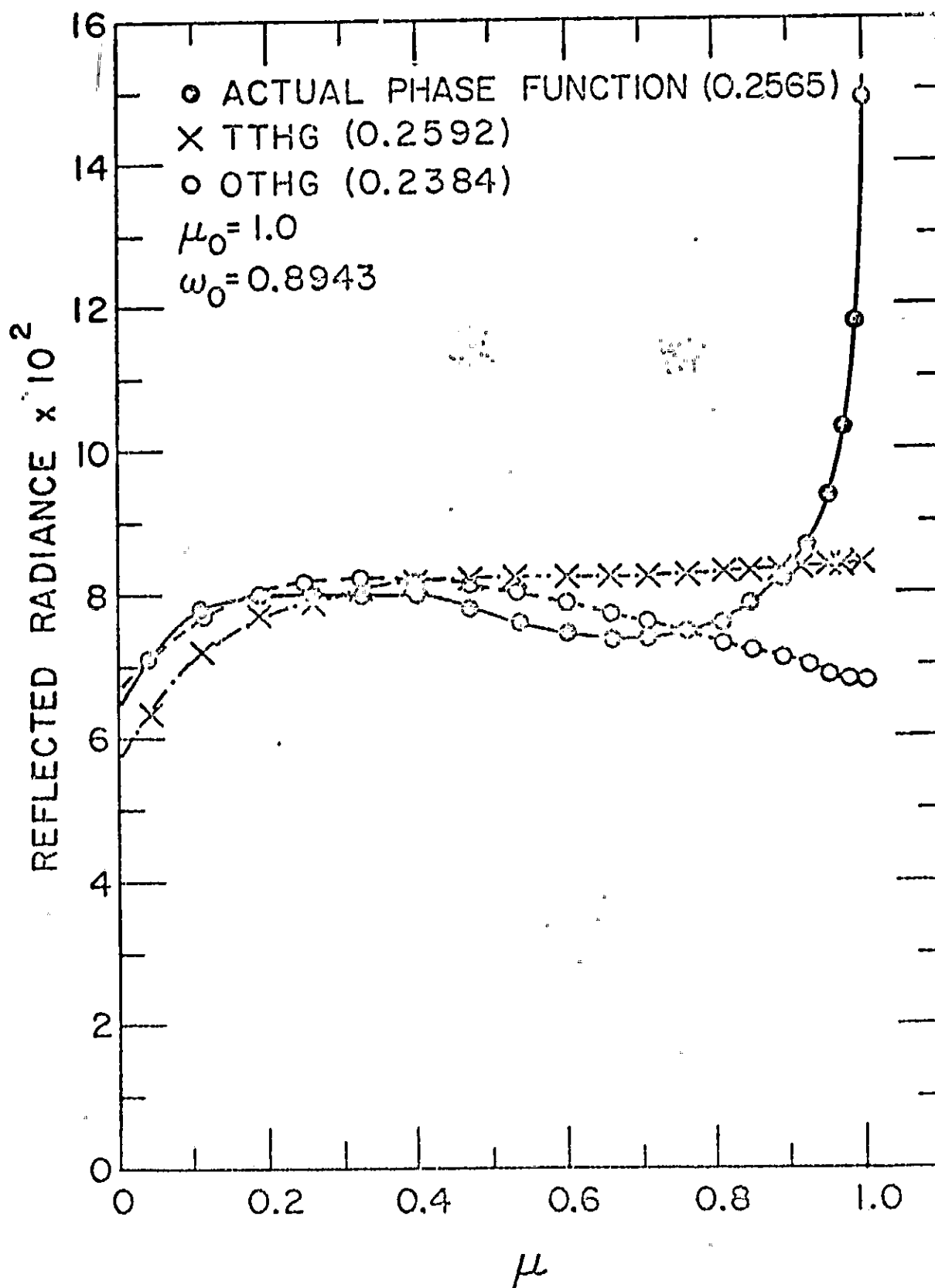


Figure 10

Figure 11

